Journal of Chromatography, 132 (1977) 387–397

CHROM. 9734

GENERAL PERMEATION CHROMATOGRAPHY EQUATION AND ITS APPLICATION TO TAYLOR-MADE CONTROLLED PORE GLASS COLUMNS

W. HALLER*, A. M. BASEDOW and B. KÖNIG
Institute for Applied Physical Chemistry, University of Heidelberg, Heidelberg (G.F.R.)
(Received July 2nd, 1976)

SUMMARY

Permeation chromatography of narrow molecular weight dextrans ranging in weight from 1000 to 300,000 daltons was performed on columns of controlled pore glass. In contrast to wide-pore substrates, the K *vs.* log M plots are monotonic, except for a short "upturn" of the curve for small values of K. The experimental results for all dextrans and poresizes obey a relatively simple general equation between $K = 0.25$ and 1.00.

An expansion of the equation, allowing for width of pore size distribution extends the experimental fit of the equation to below $K = 0.25$ and demonstrates that the fundamental separation mechanism is not the result of a spectrum of pore sizes.

The general equation is useful for pore size selection and for the design of composite systems used in the analysis of mixtures spanning wide molecular weight ranges.

INTRODUCTION

Through extensive fractionation and characterization work previously performed by Basedow *et al.* extremely narrow dextran fractions have become available[1]. These fractions were investigated by ultracentrifuge and end-group analysis, as well as by controlled pore glass (CPG) chromatography[2]. They reveal M_w/M_n values around 1.06. In contrast to this, the usual commercial dextran fractions have a M_w/M_n value of 1.35.

Fig. 1 (from ref. 3) shows the molecular weight distribution in a commercial clinical dextran of nominal molecular weight of 40,000 daltons. While the M_w of 35,600 daltons is fairly close to the nominal value, the "most probable" weight (M_0) of 25,000 daltons is approximately 60% of the nominal weight. This explains the apparent discrepancy between different studies undertaken with such broad fractions.

The general implications of exact molecular weight distribution for the

* To whom reprint requests should be directed (Permanent address: National Bureau of Standards, Washington, D.C. 20234, U.S.A.)

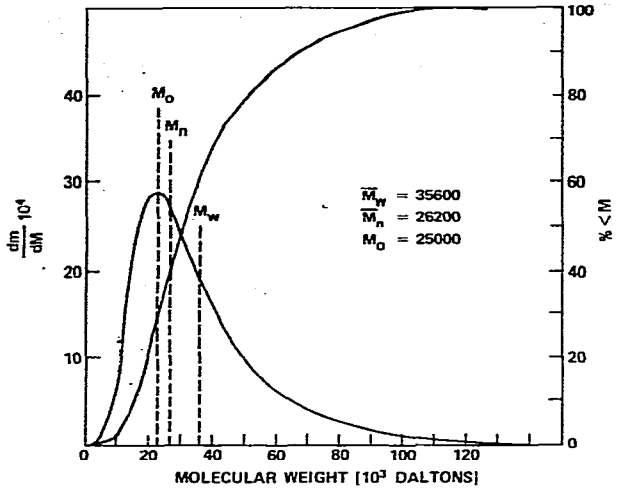

Fig. 1. Differential and integral molecular weight distribution curves of a clinical dextran of 40,000 nominal molecular weight[3].

physical chemistry of high polymers and specifically for the medically important biopolymer dextran[3] have been well recognized. In the present work, the authors have taken advantage of the availability of the narrow, well characterized fractions and have used them as a model of an "ideal" high polymer in this chromatographic study.

It is customary to display the elution behavior of substances belonging to a homologous series in a log molecular weight *versus* elution coefficient plot. The functions along both axes do justice to the expected experimental errors and have direct interest to the scientist using permeation chromatography as a tool. The curves for various classes of substances and of porous substrates are generally s-shaped with more or less "straight" portions around the inversion point. There are presently no chromatographic theories which prima facie predict straight-line curves. The limited straightness, as useful as it may be, is fortuitous for this plotting habit. Previous work with CPG produced K *vs.* log M curves of exceptional straightness with no or only a short upturn at low K values[4,5]. It was observed that absence of upturn was found in "good", *i.e.*, extremely narrow pore distribution CPG[4]. Since the substances in the last cited work were protein sodium dodecylsulfate micelles, generalizations were not possible as the dimensions and structure of micelles follow unusual architectural patterns.

Dextrans belong to the most ideal group of polymers, consisting solely of carbohydrate chains without strongly charged groups. In aqueous solvents, their theta point is around room temperature. Similar claims of ideality can be made for CPG as substrate for permeation chromatography. In contrast to gels, its rigidity provides reproducibility and enables its pore size to be determined by electron microscopy and mercury intrusion analysis[2]. For this reason, it was used in numerous investigations into the mechanism of permeation chromatography[6–11], where its known pore size and size distribution reduced the degree of freedom of parameter adjustments to fit experimental data to theories. Dextrans had already been chromatographed on CPG by Haller[12] and by Basedow *et al.*[1], except that Haller had used

the broadly disperse dextran fractions of the trade and Basedow had mixed various CPG pore sizes in his column.

EXPERIMENTAL

Materials

Dextrans. Dextrans used in this study were prepared and characterized as described in ref. 1 and are tabulated in Table I. Fraction No. 4 was not measured in the present work because of its molecular weight being close to fraction No. 5. $\bar{M}_w$ and $\bar{M}_n$ are the molecular weights from ultracentrifuge equilibrium determinations and end-group analysis, respectively. The molecular weight average $\bar{M}_w$ is believed to be accurate within $\pm 1.5\%$. The dextrans, stored dry, had been precipitated with alcohol from their aqueous solutions and subsequently dried. To save material, a few dry granules only were dissolved before an experiment and it was found that this leads to some scatter of results. Apparently, the precipitation of already highly monodisperse samples results in further fractionation and disproportionation into granules with slightly higher or lower molecular weight. Even though this was observed, the practice of dissolving single granules only was continued for reasons of economy.

TABLE I

NARROW MOLECULAR WEIGHT DISTRIBUTION DEXTRANS

Fraction No.	$\bar{M}_w$ *(daltons)*	$\bar{M}_n$ *(daltons)*	$\bar{M}_w/\bar{M}_n$
1	287 000	286 000	1.003
2	163 000	145 000	1.124
3	74 000	73 200	1.022
4	54 100	51 000	1.061
5	51 400	48 000	1.071
6	30 200	29 900	1.010
7	22 400	22 100	1.014
8	16 800	16 000	1.050
9	13 100	12 400	1.056
10	8 540	8 150	1.048
11	5 700	5 400	1.056
12	3 330	3 050	1.092
13	2 650	2 400	1.104
14	1 860	1 570	1.185
15	1 000	990	1.010

Controlled pore glass. Five different porous glasses were used in this study. They were prepared as described elsewhere[2]. All glasses were in the form of irregular particles in the range between 75 and 125 μm (120–200 mesh ASTM sieve size). The glasses were characterized by mercury intrusion pore size analysis. Average pore size ($P_{0.5}$) and pore diameter distribution (PD) were determined from the intrusion plots as defined in ref. 2. $P_{0.5}$ and PD in Table II are from one laboratory. Later re-runs by the same laboratory and one other laboratory gave values which were up to 5% above those given in the table.

TABLE II

CONTROLLED PORE GLASSES

Average pore diameter, $P_{0.5}$ (Å)	*Pore size distribution, PD (±%)*
84	13.0
159	4.5
227	3.9
314	4.7
517	3.4

Eluant and dextran solvent. Eluant for all chromatographic runs was an aqueous 0.1 *M* glycine buffer containing 0.076 *M* NaCl and 0.005% Na azide which was adjusted with NaOH to a pH of 8.2. Dextran solutions, 1 mg dextran per ml in the same buffer, were injected into the chromatographic columns. Buffers were de-gassed by very brief boiling before use on the columns. Buffers could be stored for up to two weeks without de-gassing, if not agitated by shaking or pouring. Appearance of gas bubbles in the system or bubble spikes in the monitor were taken as a signal for freshly de-gassing the eluant. Freshly de-gassed buffer was stored in a reservoir flask and transferred by hose rather than by pouring to the eluant delivery burette.

Equipment

The chromatographic system is shown in Fig. 2. A low pulsating peristaltic pump was used for eluant transport. A wide variability in flow-rate is particularly

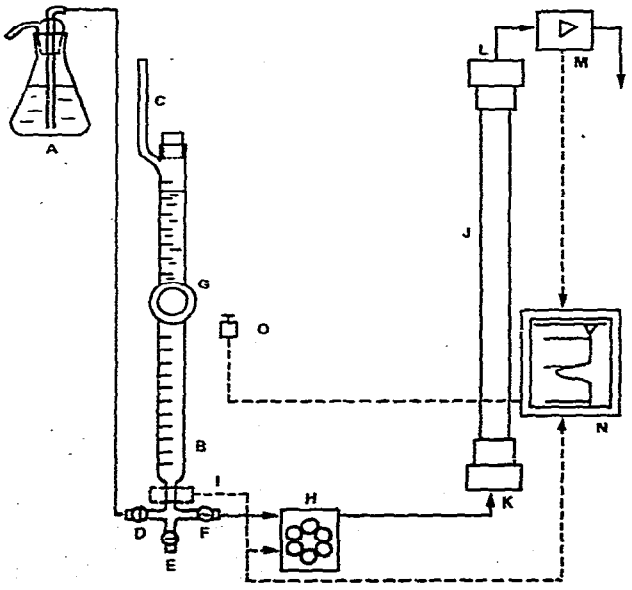

Fig. 2. Chromatographic system. (A) Eluant reservoir; (B) eluant burette; (C) level tube; (D, E, F) stopcocks; (G) magnifier; (H) peristaltic pump; (I) photoelectric shut-off; (J) column; (K, L) septum ports; (M) monitor; (N) recorder; (O) event marker.

useful for fast orientation runs, fast flushing of the column, and dissolving of air in the column in case such had been admitted by mistake. To avoid such accidents, a photoelectric eluant monitor is provided.

The chromatographic columns were of a commercial cartridge type design[13], which permitted the porous glass to be permanently locked between two porous stainless-steel disks. The columns had rubber septa ports. When well packed, the bed or porous glass does subsequently not change its volume. Therefore, no movable piston design was necessary. Columns were slurry packed (in de-gassed water) using an orbital column vibrator. Usually 2 h of strong vibration with occasional strong tapping of the column to break up possible bridging produced columns of an exclusion volume (V_0) of 38.8–43.3% of column volume. The column with a V_0 larger than 42% showed distinctly wider peaks, which was, however, of no particular detriment in this study. Columns were weighed empty, filled with water, and after packing was completed. The CPG was also weighed (dry) before the slurry was made and unused slurry was dried and the weight of excess CPG determined. From this, the actual weight (dry) of CPG in the column was calculated. The total volume of water in a packed column (V_t) was calculated from subtracting the dry CPG weight from the weight of the packing (packed weight minus empty weight).

Both column ends were connected via hypodermic needles to the eluant lines. Needles of 0.6 mm outer diameter were used. Syringes with the same type needle were used for injecting of samples. To prevent coring of the septa and the bending of the needle-bevel into an injurious outward hook, the bevels were slightly bent towards the needle center before use. Thus, septa endured several hundreds of perforations.

The monitor was a recording refractometer with reference cell and eluograms were produced with a multiple paper speed millivolt recorder. Occasional observation of the burette and marking of a particular volume on the paper by shortening the millivolt input with a hand switch was used to correlate time, volume, and paper transport. All peak position readings were corrected by adding to them the volume of the injected sample and by subtracting the volume between column exit and monitor cell. The latter volume was experimentally determined by injecting a very small volume of a salt solution through the exit septum of the column and measuring the elution volume until the peak appeared on the recording. Column dimensions were either 750 × 8 mm I.D. or 1000 × 11 mm I.D.

Procedure

The exclusion volume (V_0) of all columns was calibrated with a tobacco mosaic solution before use. The same volume of tobacco mosaic virus or dextran solution was injected in all cases. The injected amounts were 0.5 ml for the 8-mm columns and 1.0 ml for the 11-cm columns. It was determined in preliminary experiments that reducing the injection volume below these amounts did not reduce the peak broadening. Injecting too small volumes of highly concentrated solutions resulted in peak tailing.

Peak shift and peak broadening as a function of eluant flow-rate were investigated in preliminary experiments. Peaks come slightly earlier[12] at high flow velocities. As a result of these experiments, flow-rates were chosen which gave no further peak shift when the flow-rate was further reduced. These velocities were 15 ml/h for the 8-mm and 30 ml/h for the 11-mm columns. At such speed, a typical column of

103.4 ml envelope size had tobacco mosaic and glucose peaks at 40.2 and 82.4 ml, respectively. The broadness (σ) of these peaks was 1.2 and 1.57 ml, from which HETPs of 0.89 and 0.36 mm can be calculated.

RESULTS AND DISCUSSION

The elution volumes V_e of all dextrans were determined, and correlated for sample volume and system delay as described before. The corrected V_e was then normalized[14] with respect to V_0 (from TMV calibration) and V_t (from weight data during column packing) according to $K = (V_e - V_0)/(V_t - V_0)$. The experimental results are summarized in Fig. 3.

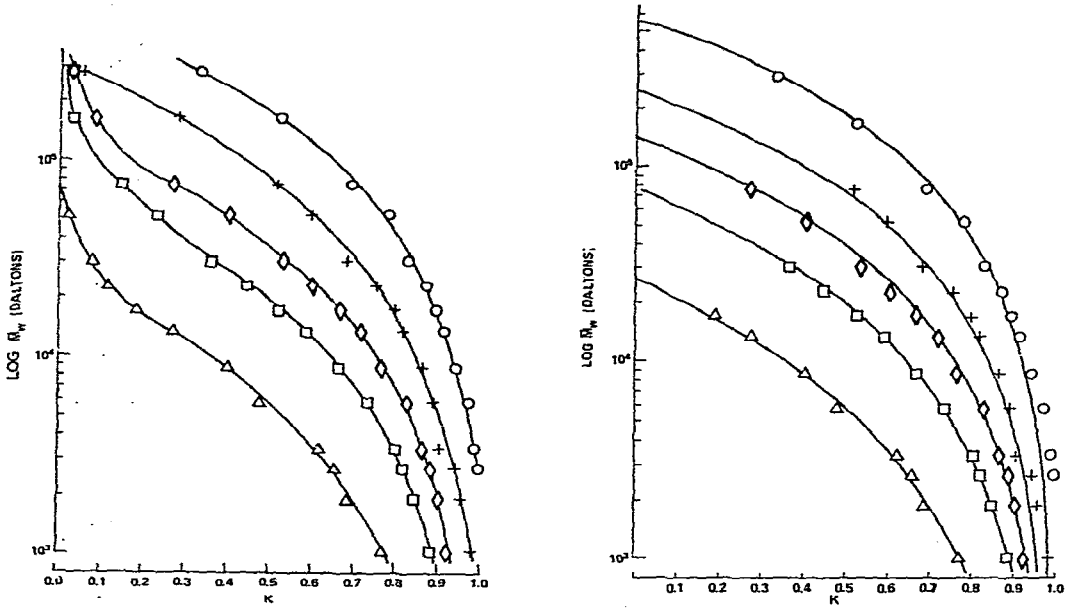

Fig. 3. Normalized elution volume K *vs.* log of molecular weight ($\bar{M}_w$) of narrow molecular weight distribution dextran. Average pore diameters $P_{0.5}$ (Å): △, 84; □, 159; ◇, 227; +, 314; ○, 517.

Fig. 4. Experimental data and curves for eqn. 8. (Symbols as in Fig. 3).

It is obvious from Fig. 3 that K *vs.* log M curves are monotonic, except for a short "upturn" for low K values. Such "upturns" are much more pronounced in gels with their wide pore size distribution. It was also observed in this and previous[4] work with CPG that the magnitude of this upturn is related to pore size distribution, with glass of very narrow distribution having no "upturn" at low K and, thus, the flattest (highest resolution) K *vs.* log M curve for this region.

In view of the above, it was first attempted to device an empirical equation with a minimum of variable parameters which describes the elution behavior in the region of monotony between $K = 0.25$ and 1.0. Such an equation assumes a totally monodisperse CPG. This equation was then expanded for a finite distribution of pores extending it to experimental values below $K = 0.25$.

The basic assumption of the derived equation is that the elution constant K depends primarily on the ratio D/P_e, where D is the dimension of the molecule governing its penetration of the pores and P_e the effective pore diameter of the porous glass. Such an equation has the form

$$\left(\frac{D}{P_e}\right)^N = 1 - K \tag{1}$$

For high polymers holds furthermore the general power law

$$D = a\bar{M}_w^{\,b} \tag{2}$$

whereby a and b depend on conformation in solution of the particular high polymer.

In the present work it was found that N, although close to 1, varies significantly with the pore size according to

$$N = dP_e^{\,c} \tag{3}$$

By multiple regression analysis of the experimental data (excluding these for $K < 0.25$), values, for the introduced constants were found to be

$$a = 0.215;\ b = 0.587;\ c = 0.164;\ d = 0.375 \tag{4}$$

Combining eqns. 1, 2, and 3, and solving for K, one obtains

$$K = 1 - \left(\frac{a\bar{M}_w^{\,b}}{P_e}\right)^{dP_e^c} \tag{5}$$

After introducing (log $\bar{M}_w$) by

$$\bar{M}_w^{\,b} = 10^{b \log \bar{M}_w} \tag{6}$$

one obtains

$$K = 1 - \left(\frac{a\,10^{b \log \bar{M}_w}}{P_e}\right)^{dP_e^c} \tag{7}$$

By further introducing the values a, b, c, and d (eqn. 4), one obtains

$$K = 1 - \left(\frac{0.215 \cdot 10^{0.587 \log \bar{M}_w}}{P_e}\right)^{0.375\, P_e^{0.164}} \tag{8}$$

For the purpose of this part of the data treatment, it is assumed that P_e is identical with the mean pore diameter $P_{0.5}$ from mercury intrusion (Table II). Fig. 4 shows the curves for eqn. 8 for five different pore sizes and also the points for the corresponding experimental data. As previously explained, values below $K = 0.25$ have been omitted.

Expanded general equation

The good agreement of eqn. 5 with experimental data in spite of the simplifying assumption of an absolute sharp pore distribution can be explained by the fact that for the largest part of the resolution curve range self compensation exists. In other words, looking at the substrate as a mixture of substrates with larger and smaller pores, one obtains a series of slightly shifted resolution curves, but the sum average of these resolution curves corresponds closely to the theoretical curve for the average pore size $P_{0.5}$. This type of averaging, however, does not apply to low K values when the molecular diameter D becomes so large that the molecules start to penetrate only the larger part of the pore spectrum. In this case, the P_e shifts away from $P_{0.5}$ towards a new larger pore size average which excludes the smaller pores, which have now become inaccessible to the species. This is the range of the upturn of the resolution curves. That, in the case of controlled pore glass, this happens so close to $K = 0$ is due to the very sharp pore distribution of this material. The above considerations, explaining the upturn for low K values, are similar to the one previously used to explain the total mechanism of permeation chromatography of gels[15]. In view of the very wide pore distribution of gels, this seems well justified and, at least for gels, a considerable contributing factor. In CPG, it is now recognized that finite pore distribution contributes only to the "upturn". That CPG still sorts molecules by sizes rather than by a digital sieving effect speaks for a basic mechanism which does not rely upon a distribution of pore sizes.

For the following it is now assumed that the pores of CPG are distributed in a logarithmic gaussian distribution around the mean pore size value $P_{0.5}$. The integral of such a distribution is the error function $y = \mathrm{erf}\, x$, where

$$x = (\log P_e - \log P_{0.5})/\sigma \tag{9}$$

and y the fraction of total pore volume. If all the pores are accessible, the mean is $x = 0$ and $P_e = P_{0.5}$. If some of the smaller pores become not accessible because their size is below that of the species D, the effective mean becomes P_e, which is the pore size at one-half of the residual available pore spectrum (see Fig. 5). Analytically, the new effective pore size P_e can be calculated as

$$\log P_e = \log P_{0.5} + \sigma \mathrm{erf}^{-1}\left[\frac{1 + \mathrm{erf}\dfrac{(\log P_{\mathrm{lim}} - \log P_{0.5})}{\sigma}}{2}\right] \tag{10}$$

whereby

$$\log P_{\mathrm{lim}} = \log D = \log a + b \log M \text{ (from eqn. 2).}$$

Calculating P_e from eqn. 10 and substituting in eqn. 8 accounts for pore distribution and produces an upturn in the resolution curve. This is demonstrated in Fig. 6. This also shows that for a σ of zero, P_e becomes equal to $P_{0.5}$ and one obtains the curves of Fig. 4.

Fig. 7 shows curves according to eqns. 8 plus 10 and the corresponding experimental data. The values for σ were arrived by trial and error rather than by using the

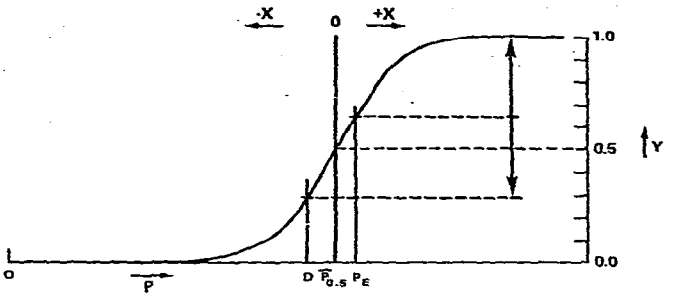

Fig. 5. Pore size distribution correction.

pore distributions (*PD*) of Table II. The true pore distribution is obviously not fully logarithmic gaussian and rather than going to more complex and unmanageable distribution functions, the σ were adjusted for best fit. The agreement is still not excellent, however, this may also be due to errors in the determination of *K*.

Application of general equation

It is expected that the above general equation will be an aid to pore size selection in such cases where one wishes to cover a particular range of molecular sizes. Since any broadening of pore size due to mixing of substrates will result in a decrease of actual resolution, it is advisable to select, whenever possible, single pore sizes covering the desired range.

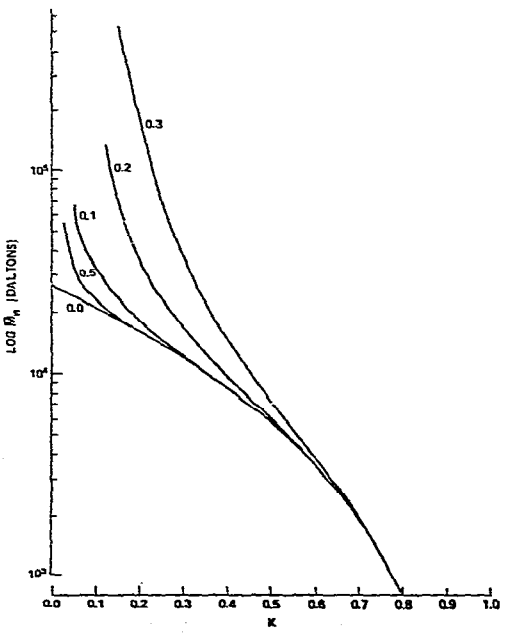

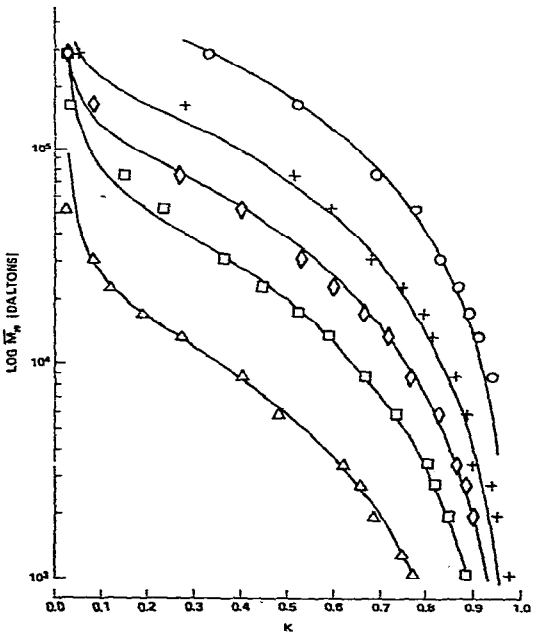

Fig. 6. Pore size distribution correction for $P_{0.5} = 84$ Å, assuming five values of σ.

Fig. 7. Curves for eqns. 8 plus 10 and experimental data. $P_{0.5}$ values for the symbols as in Fig. 3, σ values: △ and □, 0.08; ◇, 0.06; + and ○, 0.05.

In the practice of high-polymer analysis, one may, however, wish to span much larger ranges. This was done by Basedow *et al.*[1] and Basedow and Herbert[3], where seven different pore sizes had been mixed in one column in such a way that each pore size was represented by the same pore volume. Fig. 8 shows the theoretical resolution curves using eqns. 8 and 10 for the seven pore sizes. Also shown is the propotional summation of the seven curves and experimental values determined by Basedow *et al.* These experimental values are of more recent data[16] than those in refs. 1 and 3. Basedow *et al.* (see note at the end of ref. 1) have since improved their column packing technique, obtaining less peak broadening and enabling the use of much larger flow-rates. These changes are also reflected in somewhat different K *vs.* log M curves.

CONCLUSIONS

Evolving from relatively simple assumptions, an equation relating pore size, molecular weight and elution coefficient of highly monodisperse dextran was derived (eqn. 8). Allowing for width in pore size distribution, the latter equation is expanded by eqn. 10. This expansion describes and explains the non-monotonous "upturn" of the K *vs.* log $\bar{M}_w$ plot for low values of K. It also demonstrates that the basic mechanism producing elution of molecules in descending order of size is not that of a fractional exclusion from a distribution of pore sizes in the substrate. The quotient

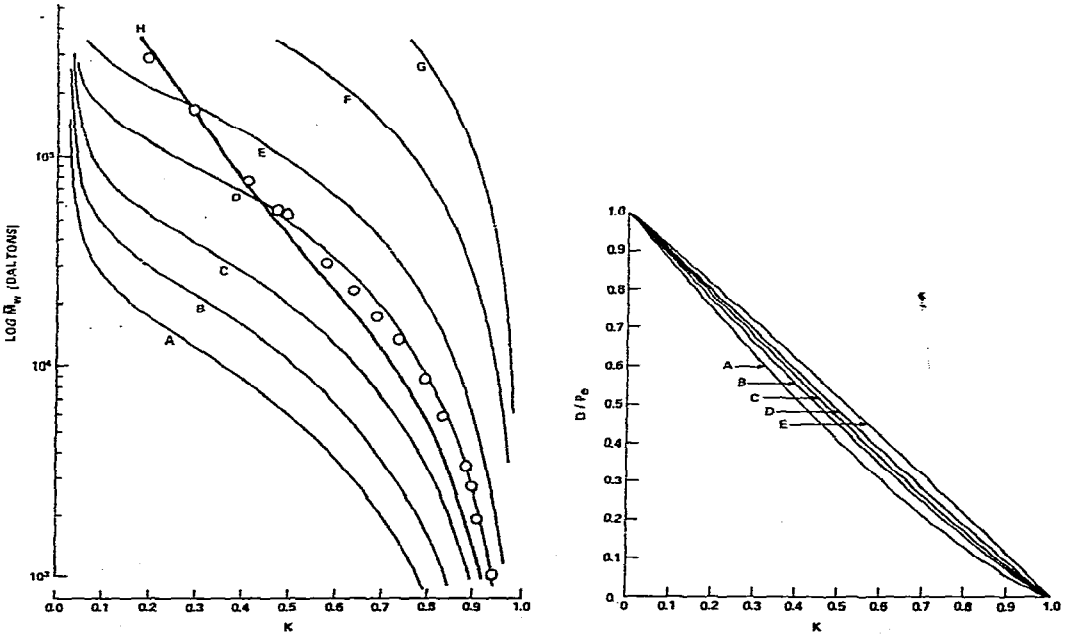

Fig. 8. Composite column having seven pore sizes. Theoretical curves for single sizes; $P_{0.5}$ (Å) values: A, 86; B, 115; C, 160; D, 254; E, 363; F, 693; G, 1250, σ values: A–C, 0.08; D, 0.06; E–G, 0.005. H, theoretical curve for mixture of sizes.

Fig. 9. Curves for the equation $K = 1 - (D/P_e)^{0.375P_e^{0.164}}$. P_e values (Å): A, 84; B, 159; C, 227; D, 314; E, 517.

D/P_e in eqn. 1 would support a mechanism based upon models of limited geometric distribution probability[17], except that these mechanism should, however, not have an N which is pore size dependent. A diffusional mechanism[18] could, however, have parameters which are not just D/P_e dependent, but also have parameters which have a pore size or species size dependent N. Fig. 9 shows solutions of eqn. 1 for several pore sizes.

The derived equations should be tested for other substances. If the size of the substance is known (or can be calculated), eqns. 1 plus 3 should be used with P_e being equal to the average pore diameter $P_{0.5}$ of the glass, providing K is above 0.25. For small K, P_e should be calculated according to eqn. 10. Parameters c and d should not be substance dependent.

For polymer series, eqn. 5 should be used, however, parameters a and b (eqn. 2) are substance dependent and may be different for other polymers. Again, eqn. 10 should be added for low values of K.

ACKNOWLEDGEMENTS

The author thanks Miss Beate Bordne for her help in obtaining and processing the experimental data. Thanks go to Professor Dr. K. H. Ebert for his interest and for making available his facilities, and to the Alexander von Humboldt Foundation for enabling the pursuit of this study.

REFERENCES

1 A. M. Basedow, K. H. Ebert, H. Ederer and H. Hunger, *Makromol. Chem.*, 177 (1976) 1501.
2 W. Haller, *Nature (London)*, 206 (1965) 693.
3 A. M. Basedow and K. H. Ebert, *Infusionstherapie*, 2 (1975) 261.
4 R. C. Collins and W. Haller, *Anal. Biochem.*, 54 (1973) 47.
5 M. J. Frenkel and R. J. Blagrove, *J. Chromatogr.*, 111 (1975) 397.
6 M. J. R. Cantow and J. F. Johnson, *J. Appl. Polym. Sci.*, 11 (1967) 1851.
7 E. F. Cassasa, *J. Phys. Chem.*, 75 (1971) 3929.
8 C. L. Deligny, *J. Chromatogr.*, 36 (1971) 50.
9 J. C. Moore and M. C. Arrington, *Int. Symp. Macromol. Chem., Tokyo and Kyoto*, Section VI (1966) 107.
10 W. W. Yau, *J. Polym. Sci., Part A2*, 7 (1969) 483.
11 G. K. Ackers, *Advan. Protein Chem.*, Academic Press, New York, 1970, p. 343.
12 W. Haller, *J. Chromatogr.*, 32 (1968) 676.
13 W. Frisch-Niggemeyer, *J. Clin. Microbiol.*, 2 (1975) 377.
14 R. M. Wheaton and W. C. Bauman, *Ann. N.Y. Acad. Sci.*, 57 (1953) 159.
15 J. Porath, *Pure Appl. Chem.*, 6 (1963) 233.
16 A. M. Basedow, unpublished results.
17 E. F. Cassasa, *J. Polymer Sci.*, B5 (1967) 773.
18 G. K. Ackers, *Biochemistry*, 3 (1964) 723.